

Singular value decomposition-based multiuser multiple-input multiple-output vector perturbation-aided downlink transmitter and lattice-reduction-assisted uplink receiver pair

W. Liu¹ C. Li² J.-D. Li¹ L. Hanzo³

¹State Key Laboratory of ISN, Xidian University, Xian, Shaanxi 710071, People's Republic of China

²School of Computer and Technology, Xi'an University of Posts and Telecommunications, Xian, Shaanxi 710061, People's Republic of China

³School of ECS, University of Southampton, Southampton SO17 1BJ, UK

E-mail: lh@ecs.soton.ac.uk

Abstract: A full-duplex uplink/downlink (UL/DL) system having a UL transmitter/receiver (transceiver) pair and a DL transceiver is considered. Both the UL and DL are improved. The DL is enhanced by a novel vector perturbation (VP)-aided singular value decomposition (SVD)-based precoding scheme, which is capable of exploiting the different-quality SVD eigenbeams and substantially reduces the overall average transmit power requirement of the traditional zero-forcing (ZF) precoder. By contrast, the UL is enhanced by a lattice reduction (LR)-aided receiver scheme designed for SVD-based multiuser multiple-input multiple-output (MU MIMO) UL transmission, when different modulation schemes are employed for different-quality eigenbeams. This new UL scheme avoids the noise-enhancement problem of the classic ZF UL receiver. The authors demonstrate that the proposed VP-aided DL and LR-assisted UL constitute a powerful full-duplex system, which achieves an ~ 15 dB signal to noise ratio (SNR) gain for both SVD-based MU-MIMO DL and UL transmissions over the traditional ZF-aided schemes at a bit error rate (BER) of 10^{-3} .

1 Introduction

Multiple-input multiple-output (MIMO) antenna configurations are capable of significantly increasing the spectral efficiency of a single-user link [1]; however, the performance of multiuser (MU) MIMO systems is partially eroded by the multiple user interference (MUI) imposed in the downlink (DL) and by the multiple access interference (MAI) in the uplink (UL) transmissions.

Assuming that the DL channel state information (CSI) about to be encountered is available at the base station (BS), – which can be obtained by sophisticated channel estimation algorithms at the mobile stations (MSs) and then feedback to the BS after quantisation, – DL transmit preprocessing techniques can be used to mitigate the MUI for MU-MIMO DL transmission [2]. These methods are also often referred to as multiuser transmission (MUT), where we generate unique, user-specific DL signals for each MS by exploiting their unique, user-specific CSI. The system performance attainable with the aid of multiple transmit and multiple receiver antennas was substantially improved in [3], which resulted in the novel concept of joint transmitter/receiver (transceiver) design for MU MIMO systems [3]. A singular value decomposition (SVD)-based DL MU-MIMO eigenmode transmission-aided joint

transceiver pair was proposed in [4], which is capable of completely eliminating the MUI and also supports the employment of adaptive modulation for different-quality eigenbeams. However, in the SVD-based DL joint transceiver of [4], the low-complexity zero-forcing (ZF) DL precoder was invoked at the BS, which typically results in relatively poor performance. As a remedy, the more sophisticated vector perturbation (VP)-based algorithm of [5] was proposed for improving the attainable system performance. However, the VP-based MUT scheme of [5] employs the same modulation scheme for all virtual parallel links, although in the SVD-based DL MUT scheme [4], ideally different modulation schemes should be used for different-quality parallel DL eigenmodes.

In contrast to the above-mentioned DL scenario, as far as UL multiuser detection (MUD) is concerned, the joint UL transceiver design philosophy can be also used to improve the attainable UL system performance [6], provided that an accurate CSI is available at the MSs. As a counterpart, the SVD-based eigenmode UL multi-stream transmission concept was proposed in [4]. However, in the SVD-based UL joint transceiver [4], the ZF UL receiver is used at the BS, which results in noise-enhancement and hence degrades the system performance. The lattice reduction (LR)-aided concept was proposed for mitigating the effects of noise

enhancement [7], which has the potential of significantly improving the achievable system performance. However, the LR-based detection scheme of [7] was designed for supporting the same modulation scheme in all virtual parallel links, although in the SVD-based UL transmission scheme [4], ideally different modulation schemes would be used for different-quality parallel eigenmodes.

Against this background, a full-duplex UL/DL system having an improved UL and DL transceiver pair is considered. More explicitly, the DL is enhanced by a new VP-aided SVD-based transmitter, which is capable of supporting different modulation schemes for different-quality parallel virtual DL streams. By contrast, the UL is enhanced by a novel LR-based UL receiver scheme, which is capable of detecting the different UL modulation schemes of the different-quality SVD eigenbeams.

This treatise is structured as follows. In Section 2, we briefly review the traditional SVD-based joint DL transceiver scheme and propose a novel VP-aided SVD-based joint DL transceiver scheme. In Section 3 the traditional SVD-based joint UL transceiver arrangement is reviewed and a novel LR-aided UL receiver is proposed, which avoids the noise-amplification problem of the ZF receiver and it is capable of detecting the different modulation schemes of the different-quality SVD eigenbeams. Our simulation results are provided in Section 4, and our conclusions are offered in Section 5.

2 SVD-based VP-aided MU-MIMO DL transmission

2.1 System model

The MU-MIMO DL system considered in this section is shown in Fig. 1, where a single BS supports K MSs. The BS is equipped with M DL transmit antennas and the k th MS is equipped with N_k DL receive antennas.

Let the $(n_k \leq N_k)$ -component DL symbol vector \mathbf{x}_k to be transmitted to the k th MS be expressed as

$$\mathbf{x}_k = [\mathbf{x}_{k1}, \mathbf{x}_{k2}, \dots, \mathbf{x}_{kn_k}]^T \quad (1)$$

As shown in Fig. 1, \mathbf{x}_k is preprocessed by an $(M \times n_k)$ -component preprocessing matrix \mathbf{P}_k , yielding

$$\mathbf{d}_k = \mathbf{P}_k \boldsymbol{\beta}_k \mathbf{x}_k, \quad k = 1, 2, \dots, K \quad (2)$$

where $\boldsymbol{\beta}_k$ is an $(n_k \times n_k)$ -dimensional diagonal matrix, which is given by

$$\boldsymbol{\beta}_k = \text{diag}[\beta_{k1}, \dots, \beta_{kn_k}] \quad (3)$$

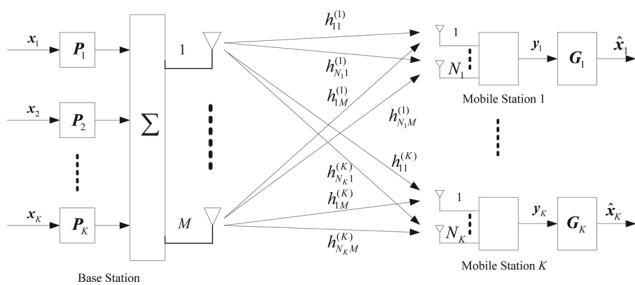


Fig. 1 Schematic of MU-MIMO DL transmission using both preprocessing and postprocessing

where β_{kn_i} is the power scaling coefficient, normalising the transmission power for the i th symbol x_{ki} of the k th MS. The M -component DL-transmitted signal vector \mathbf{d} of the BS can be expressed as

$$\mathbf{d} = \sum_{k=1}^K \mathbf{d}_k = \sum_{k=1}^K \mathbf{P}_k \boldsymbol{\beta}_k \mathbf{x}_k = \mathbf{P} \boldsymbol{\beta} \mathbf{x} \quad (4)$$

where \mathbf{P} is an $(M \times \sum_{k=1}^K n_k)$ -component matrix given by

$$\mathbf{P} = [\mathbf{P}_1, \mathbf{P}_2, \dots, \mathbf{P}_K] \quad (5)$$

and \mathbf{x} is a $(\sum_{k=1}^K n_k)$ -component vector containing the transmitted data, which is given by

$$\mathbf{x} = [\mathbf{x}_1^T, \mathbf{x}_2^T, \dots, \mathbf{x}_K^T]^T \quad (6)$$

Furthermore, $\boldsymbol{\beta}$ is a $(\sum_{k=1}^K n_k \times \sum_{k=1}^K n_k)$ -dimensional power scaling matrix, which is given by

$$\boldsymbol{\beta} = \text{diag}[\boldsymbol{\beta}_1, \dots, \boldsymbol{\beta}_K] \quad (7)$$

Assuming a flat-fading channel, the $(N_k \times M)$ -component DL channel coefficient matrix \mathbf{H}_k^{DL} between the M transmit antennas of the BS and the N_k receive antennas of the k th MS is given by

$$\mathbf{H}_k^{\text{DL}} = \begin{bmatrix} h_{11}^{(k)} & h_{12}^{(k)} & \dots & h_{1M}^{(k)} \\ h_{21}^{(k)} & h_{22}^{(k)} & \dots & h_{2M}^{(k)} \\ \vdots & \vdots & \ddots & \vdots \\ h_{N_k 1}^{(k)} & h_{N_k 2}^{(k)} & \dots & h_{N_k M}^{(k)} \end{bmatrix} \quad (8)$$

where $h_{mn}^{(k)}$ denotes the DL channel coefficient between the n th transmit antenna of the BS and the m th receive antenna of the k th MS. The N_k -component received signal vector \mathbf{y}_k of the k th MS can be expressed as

$$\mathbf{y}_k = \mathbf{H}_k^{\text{DL}} \mathbf{d} + \mathbf{n}_k = \mathbf{H}_k^{\text{DL}} \mathbf{P} \boldsymbol{\beta} \mathbf{x} + \mathbf{n}_k, \quad k = 1, 2, \dots, K \quad (9)$$

where \mathbf{n}_k is an N_k -element AWGN vector having a zero mean and a covariance matrix of $\sigma^2 \mathbf{I}_{N_k}$. Assuming $M \geq N_k$, the SVD of \mathbf{H}_k^{DL} can be expressed as

$$\mathbf{H}_k^{\text{DL}} = \mathbf{U}_k [\boldsymbol{\Lambda}_k^{1/2}, \mathbf{0}] \mathbf{V}_k^H \quad (10)$$

where \mathbf{U}_k is an $(N_k \times N_k)$ -component unitary matrix, consisting of the N_k left singular vectors of \mathbf{H}_k^{DL} and \mathbf{V}_k is an $(N_k \times N_k)$ -component unitary matrix, consisting of the M right singular vectors of \mathbf{H}_k^{DL} . Furthermore, $\boldsymbol{\Lambda}_k = \text{diag}\{\lambda_{k1}, \lambda_{k2}, \dots, \lambda_{kN_k}\}$ is an $(N_k \times N_k)$ -component diagonal matrix containing the eigenvalues of $\mathbf{H}_k^{\text{DL}} (\mathbf{H}_k^{\text{DL}})^H$ and having diagonal elements arranged in a non-increasing order. Upon substituting (10) into (9), the DL-received signal \mathbf{y}_k of the k th MS seen in Fig. 1 may be expressed as

$$\mathbf{y}_k = \mathbf{U}_k \boldsymbol{\Lambda}_k^{1/2} \mathbf{V}_k^H \mathbf{P} \boldsymbol{\beta} \mathbf{x} + \mathbf{n}_k, \quad k = 1, 2, \dots, K \quad (11)$$

For the traditional SVD-based joint DL MUT scheme of [4], the $(n_k \times N_k)$ -element postprocessing matrix \mathbf{G}_k seen in Fig. 1

was chosen to be [4]

$$\mathbf{G}_k = \mathbf{U}_{kn_k}^H \quad (12)$$

where \mathbf{U}_{kn_k} consists of the first n_k columns of \mathbf{U}_k . Correspondingly, the decision vector \mathbf{x}_k is given by

$$\begin{aligned} \hat{\mathbf{x}}_k &= \mathbf{G}_k \mathbf{y}_k = \mathbf{U}_{kn_k}^H \mathbf{y}_k = \Lambda_{kn_k}^{1/2} \mathbf{V}_{kn_k}^H \mathbf{P} \boldsymbol{\beta} \mathbf{x} + \mathbf{U}_{kn_k} \mathbf{n}_k \\ &= \Lambda_{kn_k}^{1/2} \mathbf{V}_{kn_k}^H \mathbf{P} \boldsymbol{\beta} \mathbf{x} + \hat{\mathbf{n}}_k, \quad k = 1, 2, \dots, K \end{aligned} \quad (13)$$

where $\Lambda_{kn_k}^{1/2}$ is an $(n_k \times n_k)$ -dimensional diagonal matrix, consisting of the first n_k diagonal elements of $\Lambda_k^{1/2}$, whereas \mathbf{V}_{kn_k} is an $(M \times n_k)$ -dimensional matrix, comprising the first n_k columns of \mathbf{V}_{sk} . Furthermore, $\hat{\mathbf{n}}_k = \mathbf{U}_{kn_k} \mathbf{n}_k$ in (13) is an AWGN noise vector with a zero mean and a covariance matrix of $\sigma^2 \mathbf{I}_{n_k}$.

The decision vector $\hat{\mathbf{x}}$ for all the K MSs is expressed as

$$\hat{\mathbf{x}} = [\hat{\mathbf{x}}_1^T, \hat{\mathbf{x}}_2^T, \dots, \hat{\mathbf{x}}_K^T]^T = \Lambda^{1/2} \mathbf{V}_s^H \mathbf{P} \mathbf{x} + \mathbf{n} \quad (14)$$

where we have

$$\begin{aligned} \Lambda &= \text{diag}\{\Lambda_{1n_1}, \Lambda_{2n_2}, \dots, \Lambda_{Kn_K}\} \\ \mathbf{V}_s &= [\mathbf{V}_{1n_1}, \mathbf{V}_{2n_2}, \dots, \mathbf{V}_{Kn_K}] \\ \mathbf{n} &= [\hat{\mathbf{n}}_1^T, \hat{\mathbf{n}}_2^T, \dots, \hat{\mathbf{n}}_K^T]^T \end{aligned} \quad (15)$$

For the traditional SVD-based joint DL MUT transceiver, the preprocessing matrix \mathbf{P} is given by Liu *et al.* [4]

$$\mathbf{P} = [\mathbf{V}_s^H]^+ = \mathbf{V}_s [\mathbf{V}_s^H \mathbf{V}_s]^{-1} \quad (16)$$

where $[\cdot]^+$ denotes the pseudo inverse of a matrix.

Assuming that the total transmit power of the BS is P_t , the power control coefficient α is introduced to meet the instantaneous power constraint of the BS, which is given by

$$\alpha = \frac{\|\mathbf{P} \boldsymbol{\beta} \mathbf{x}\|^2}{P_t} \quad (17)$$

Finally, the DL-transmitted signal vector \mathbf{d} of the BS is given by

$$\mathbf{d} = \frac{\mathbf{P} \boldsymbol{\beta} \mathbf{x}}{\sqrt{\alpha}} \quad (18)$$

The vector of the estimated signal for the k th MS is given by

$$\hat{\mathbf{x}}_k = \frac{1}{\sqrt{\alpha}} \Lambda_{kn_k}^{1/2} \boldsymbol{\beta}_k \mathbf{x}_k + \mathbf{U}_{kn_k} \mathbf{n}_k, \quad k = 1, 2, \dots, K \quad (19)$$

As seen in (16), the DL-precoding matrix \mathbf{P} of the BS is chosen according to the ZF criterion for the traditional SVD-based joint MUT-aided transceiver of [4]. It is important to note that for the sake of fair comparison of the ZF and the proposed scheme, their transmit power must be the same, which is ensured by using a higher α -value for the ZF MUT. As a result, this increased α reduces the desired signal's power in (19), which may impose a significant performance loss in comparison with the VP scheme of [5]. Let us now introduce the proposed VP-based SVD DL precoder.

2.2 Proposed method

Again, for the traditional VP scheme of [5], the BS chooses the same modulation scheme for each data stream and uses a scalar τ as the VP coefficient. However, in the context of the SVD-based DL eigenmode transmission, different modulation schemes may be chosen according to different eigenvalues. There is no common VP coefficient τ that is valid for different modulation schemes. Hence, in our SVD-based VP DL transmission scheme, an n_k -dimensional perturbation vector $\boldsymbol{\tau}_k$ is proposed for the k th MS, which is given by

$$\boldsymbol{\tau}_k = [\boldsymbol{\tau}_{k1}, \dots, \boldsymbol{\tau}_{kn_k}]^T \quad (20)$$

where τ_{ki} is the VP coefficient of the data stream x_{ki} . Specifically, τ_{ki} is chosen to be $2\sqrt{M}$ for M-ary square quadrature amplitude modulation (QAM) modulation, whereas $\tau_{ki} = 2$ for BSPK modulation [8]. Correspondingly, the $(\sum_{k=1}^K n_k)$ -component perturbation vector $\boldsymbol{\tau}$, derived for all the data streams, is given by

$$\boldsymbol{\tau} = [\boldsymbol{\tau}_1^T, \dots, \boldsymbol{\tau}_K^T]^T \quad (21)$$

Once the transmitted symbol vector \mathbf{x} and the corresponding perturbation vector $\boldsymbol{\tau}$ are determined, our goal is to find a $(\sum_{k=1}^K n_k)$ -component complex-valued integer vector $\boldsymbol{\omega}$ associated with $\boldsymbol{\omega}_l = a_l + jb_l$, $l = 1, \dots, (\sum_{k=1}^K n_k)$, where $j = \sqrt{-1}$, and a_l and b_l are real-valued integers, respectively, which minimises the instantaneous power of the precoding scheme formulated as

$$\min_{\boldsymbol{\omega}} \|\mathbf{P}(\boldsymbol{\beta} \mathbf{x} + \boldsymbol{\beta} \boldsymbol{\tau} \odot \boldsymbol{\omega})\|^2 = \|\mathbf{V}_s^H \mathbf{P}(\boldsymbol{\beta} \mathbf{x} + \boldsymbol{\beta} \boldsymbol{\tau} \odot \boldsymbol{\omega})\|^2 \quad (22)$$

where \odot denotes the element-wise product. In this treatise, the optimal $\boldsymbol{\omega}$ is obtained by invoking the sphere-encoding scheme of [5]. Once the optimal $\boldsymbol{\omega}$ is determined, the power control coefficient α is given by

$$\alpha = \frac{\|\mathbf{P}(\boldsymbol{\beta} \mathbf{x} + \boldsymbol{\beta} \boldsymbol{\tau} \odot \boldsymbol{\omega})\|^2}{P_t} \quad (23)$$

The DL transmitted signal vector \mathbf{d} of the BS is given by

$$\mathbf{d} = \frac{\mathbf{P}(\boldsymbol{\beta} \mathbf{x} + \boldsymbol{\beta} \boldsymbol{\tau} \odot \boldsymbol{\omega})}{\sqrt{\alpha}} \quad (24)$$

Correspondingly, the signal vector estimated by the k th MS is given by

$$\begin{aligned} \hat{\mathbf{x}}_k &= \frac{1}{\sqrt{\alpha}} \Lambda_{kn_k}^{1/2} (\boldsymbol{\beta}_k \mathbf{x}_k + \boldsymbol{\beta}_k \boldsymbol{\tau}_k \odot \boldsymbol{\omega}_k) + \mathbf{U}_{kn_k} \mathbf{n}_k, \\ &k = 1, 2, \dots, K \end{aligned} \quad (25)$$

where $\boldsymbol{\omega}_k$ is a complex-valued integer vector corresponding to the perturbation vector $\boldsymbol{\tau}_k$.

In order to remove the effects of the perturbation, the modulo operation is invoked [5]. Specifically, for the i th element \hat{x}_{ki} of $\hat{\mathbf{x}}_k$, the signal x_{ki} estimated after the modulo

operation is given by

$$\tilde{x}_{ki} = \text{mod}_{\tau_{ki}}(\hat{x}_{ki}) = \hat{x}_{ki} - \left\lfloor \frac{\Re[\hat{x}_{ki} + \beta_{ki}\tau_{ki}/2]}{\beta_{ki}\tau_{ki}} \right\rfloor \beta_{ki}\tau_{ki} - \left\lfloor \frac{\Im[\hat{x}_{ki} + \beta_{ki}\tau_{ki}/2]}{\beta_{ki}\tau_{ki}} \right\rfloor \beta_{ki}\tau_{ki} \quad (26)$$

where $\Re[\cdot]$ and $\Im[\cdot]$ are the real and imaginary parts of the variable, respectively, and $\lfloor \cdot \rfloor$ denotes the largest integer less than or equal to its argument.

3 SVD-based lattice reduction-aided UL transmission

3.1 System model

The MU-MIMO UL transmission considered in this section is shown in Fig. 2. The configuration of the system is the same as that of the MU-MIMO DL.

Similarly, a flat fading channel is assumed. The $(N_k \times M)$ -dimensional UL channel coefficient matrix \mathbf{H}_k^{UL} between the N_k transmit antennas of the k th MS and the M receive antennas of the BS is given by

$$\mathbf{H}_k^{\text{UL}} = \begin{bmatrix} h_{11}^{(k)} & h_{12}^{(k)} & \cdots & h_{1N_k}^{(k)} \\ h_{21}^{(k)} & h_{22}^{(k)} & \cdots & h_{2N_k}^{(k)} \\ \vdots & \vdots & \ddots & \vdots \\ h_{M1}^{(k)} & h_{M2}^{(k)} & \cdots & h_{MN_k}^{(k)} \end{bmatrix} \quad k = 1, 2, \dots, K \quad (27)$$

where h_{mm}^k denotes the channel coefficient between the m th UL receiver antenna of the BS and the n th UL transmit antenna of the k th MS. The SVD of \mathbf{H}_k^{UL} is given by

$$\mathbf{H}_k^{\text{UL}} = \mathbf{U}_k \begin{bmatrix} \Lambda_k^{1/2} \\ \mathbf{0} \end{bmatrix} \mathbf{V}_k^H, \quad k = 1, 2, \dots, K \quad (28)$$

where the $(M \times M)$ -dimensional unitary matrix \mathbf{U}_k and the $(N_k \times N_k)$ -dimensional unitary matrix \mathbf{V}_k consist of the left and right singular vectors of \mathbf{H}_k^{UL} , respectively, whereas $\Lambda = \text{diag}\{\lambda_1, \lambda_2, \dots, \lambda_{N_k}\}$ contains the N_k eigenvalues of $(\mathbf{H}_k^{\text{UL}})^H \mathbf{H}_k^{\text{UL}}$ having diagonal elements arranged in a non-increasing order. The n_k -element UL data symbol vector \mathbf{x}_k intended for the BS from the k th MS is given by

$$\mathbf{x}_k = [\mathbf{x}_{k1}, \mathbf{x}_{k2}, \dots, \mathbf{x}_{kn_k}]^T, \quad k = 1, 2, \dots, K \quad (29)$$

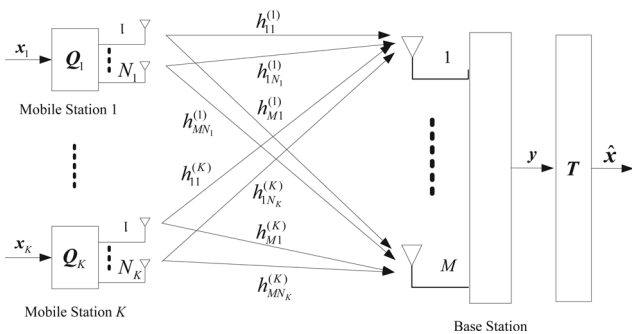


Fig. 2 Schematic of MU-MIMO UL transmission using both preprocessing and postprocessing

As shown in Fig. 2, \mathbf{x}_k is preprocessed by the transmitter preprocessing matrix \mathbf{Q}_k . For the traditional SVD-based MU-MIMO UL joint transceiver design, the preprocessing matrix \mathbf{Q}_k is set to [4]

$$\mathbf{Q}_k = \mathbf{V}_{kn_k}, \quad k = 1, 2, \dots, K \quad (30)$$

resulting in the output of

$$\mathbf{d}_k = \mathbf{V}_{kn_k} \beta_k \mathbf{x}_k, \quad k = 1, 2, \dots, K \quad (31)$$

where \mathbf{V}_{kn_k} represents the first n_k columns of \mathbf{V}_k and β_k and it is an $(n_k \times n_k)$ -dimensional diagonal matrix, which is used to normalise the transmission power of each data stream. The M -component observation vector \mathbf{y} received at the BS can be expressed as

$$\begin{aligned} \mathbf{y} &= \sum_{k=1}^K \mathbf{H}_k^{\text{UL}} \mathbf{d}_k + \mathbf{n} = \sum_{k=1}^K \mathbf{H}_k^{\text{UL}} \mathbf{V}_{kn_k} \beta_k \mathbf{x}_k + \mathbf{n} \\ &= \sum_{k=1}^K \mathbf{U}_{kn_k} \Lambda_{kn_k}^{1/2} \mathbf{V}_{kn_k} \beta_k \mathbf{x}_k + \mathbf{n} = \mathbf{U}_s \Lambda^{1/2} \beta \mathbf{x} + \mathbf{n} \end{aligned} \quad (32)$$

where \mathbf{n} is an M -component AWGN noise vector with a zero mean and a covariance matrix given by $\sigma^2 \mathbf{I}_M$. Furthermore, we have

$$\begin{aligned} \mathbf{U}_s &= [\mathbf{U}_{1n_1}, \mathbf{U}_{2n_2}, \dots, \mathbf{U}_{Kn_K}] \\ \Lambda^{1/2} &= \text{diag}\{\Lambda_{1n_1}^{1/2}, \Lambda_{2n_2}^{1/2}, \dots, \Lambda_{Kn_K}^{1/2}\} \\ \beta &= \text{diag}\{\beta_1, \beta_2, \dots, \beta_K\} \end{aligned} \quad (33)$$

For the traditional SVD-based scheme, the postprocessing matrix \mathbf{T} seen in Fig. 2 is given by [4]

$$\mathbf{T} = \mathbf{U}_s^+ \quad (34)$$

which yields the $(\sum_{k=1}^K n_k)$ -component decision vector $\hat{\mathbf{x}}$ of

$$\hat{\mathbf{x}} = \mathbf{T} \mathbf{y} = \Lambda^{1/2} \beta \mathbf{x} + \mathbf{U}_s^+ \mathbf{n} \quad (35)$$

For the traditional SVD-based UL MUD scheme of the joint transceiver, the postprocessing matrix \mathbf{T} of Fig. 2 is determined according to the ZF criterion. Owing to the non-orthogonal nature of the columns of \mathbf{U}_s , noise enhancement may be encountered, which may impose a significant performance loss.

3.2 Proposed method

It has been shown that LR-aided UL detection schemes have the potential of effectively mitigating noise enhancement [7]. However, traditional LR was conceived for detecting the same modulation scheme in all parallel streams. By contrast, in SVD-aided MU-MIMO UL transmissions different modulation schemes should be used for all parallel streams corresponding to different eigenvalues. For M -QAM, the range of the real or imaginary part of x_{ki} is $\{-\sqrt{M-1}, \dots, -1, 1, \dots, \sqrt{M-1}\}$, although for binary phase shift keying (BPSK), x_{ki} is taken from $\{-1, 1\}$. Consequently, the diagonal elements in the power scaling matrix β of (32) may be approximately configured for different modulation schemes. Furthermore, the diagonal

elements of $\Lambda^{1/2}$ in (32) are different from each other. In this case, if the traditional LR-based scheme is invoked for U_s of (32), we have

$$U_s = \hat{U}_s F^{-1} \quad (36)$$

where F is a unimodular matrix and $\hat{U}_s = U_s F$ [7], which is supposed to be near-orthogonal. The decision vector of \hat{y} based on LR is given by

$$\hat{y} = \hat{U}_s^{-1} y = F^{-1} \Lambda^{1/2} \beta x + \hat{U}_s^+ n \quad (37)$$

As \hat{U}_s is near-orthogonal, $\hat{U}_s^+ n$ is expected to impose a lower noise enhancement than $U_s^+ n$. However, since the elements of $\Lambda^{1/2} \beta$ are not integers, the elements of the resultant vector $F^{-1} \Lambda^{1/2} \beta x$ become non-integers; hence, we cannot detect the transmitted symbols correctly. In order to overcome this problem, we opted for applying the LR technique to the composite channel matrix $U_s \Lambda^{1/2} \beta$, yielding

$$U_s \Lambda^{1/2} \beta = \hat{U}_s F^{-1} \quad (38)$$

where $\hat{U}_s = U_s \Lambda^{1/2} \beta F$. The decision vector of \hat{y} is given by

$$\hat{y} = \hat{U}_s^+ y = F^{-1} x + \hat{U}_s^+ n \quad (39)$$

where the elements of the resultant vector $F^{-1} x$ are still integers.

Furthermore, let s be the vector transforming the range of $\sum_{k=1}^K n_k$ real and $\sum_{k=1}^K n_k$ imaginary parts in the transmitted symbol vector x to the same number of immediately consecutive integer [9]. Specifically, since we have $s_{kn_i} = (1 + j)$ for QAM symbols, although $s_{kn_i} = 1$ for BPSK modulation, the modified received signal vector \bar{y} can be expressed as

$$\bar{y} = \frac{1}{2} U_s \Lambda^{1/2} \beta (x - s) + \frac{1}{2} n \quad (40)$$

In this paper, the complex-valued Lenstra–Lenstra–Lovasz (LLL) algorithm is invoked for carrying out the LR transformation [9], yielding

$$\bar{y} = \frac{1}{2} \hat{U}_s F^{-1} (x - s) + \frac{1}{2} n \quad (41)$$

Consequently, the resultant decision vector \tilde{y} is given by

$$\tilde{y} = \hat{U}_s^+ \bar{y} = \frac{1}{2} F^{-1} (x - s) + \hat{U}_s^+ \frac{1}{2} n \quad (42)$$

Finally, the decision symbol vector \check{x} is given by [9]

$$\check{x} = 2F(Q(\tilde{y})) + s \quad (43)$$

which can be used for the hard-decision detection. In (43), $Q(\cdot)$ denotes the rounding operation, which rounds the real and imaginary parts of the elements in \tilde{y} to the nearest integer [9].

4 Simulation results

In this section, simulation results are provided for characterising the performance of the proposed algorithm,

where the channel coefficients are assumed to be independently and identically distributed (iid) Rayleigh fading variables. Moreover, the transmission power is $P_t = \sum_{k=1}^K n_k$ for the DL and we have $P_t = n_k$ for each MS's UL transmission. Correspondingly, the SNR per symbol is defined as $\text{SNR} = 1/\sigma^2$.

In Fig. 3, the average BER against the average SNR per symbol performance is characterised for DL transmission, when using the VP and ZF precodings, respectively. The system's configuration is shown in Table 1. Furthermore, only a single DL data stream is transmitted to each MS and a 16QAM scheme is used. We can see from Fig. 3 that the VP-based scheme significantly outperforms the traditional ZF one. When the number of transmit antennas at the BS is $M = 4$, the proposed VP-based scheme has an approximately 15 dB SNR gain over the traditional ZF scheme at the BER of 10^{-3} . Moreover, upon increasing the number of transmit antennas at the BS, the performance gain of the proposed VP scheme over the traditional ZF is reduced, because the ZF arrangement benefits more from the extra transmit diversity.

In Fig. 4, the average BER against average SNR per symbol performance is portrayed for UL transmission recorded for both the LR and ZF detection. The system configuration is shown in Table 1. Furthermore, only a single data stream is transmitted in the UL from the MS to the BS using 16QAM. As we can see from Fig. 4, the proposed LR-based scheme significantly outperforms the traditional ZF. When the number of UL receive antennas used at the BS is $M = 4$, the proposed LR-based scheme has a 16 dB SNR gain over the traditional ZF scheme at a BER of 10^{-3} . Furthermore, upon increasing the number of receiver antennas at the BS, the performance gain of the

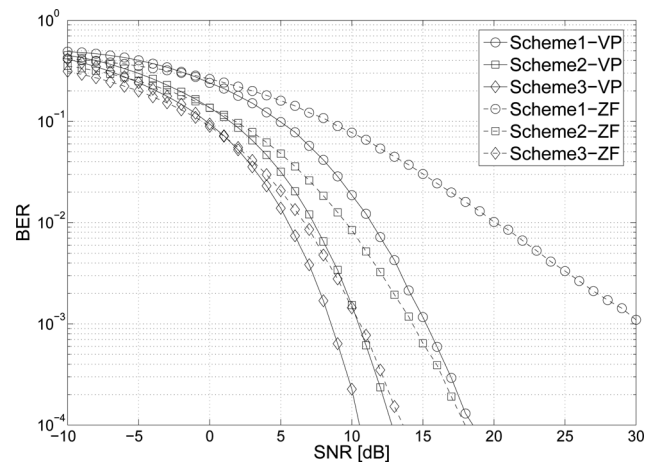


Fig. 3 Average BER against average SNR per symbol for DL transmission when using the VP and ZF precoding, respectively

System configuration is shown in Table 1. Furthermore, only a single data stream is transmitted to each of the K MSs and 16QAM is used

Table 1 Parameters for SVD-based transmission

	Scheme 1	Scheme 2	Scheme 3	Scheme 4
number of antennas at the BS (M)	4	6	8	10
number of MSs (K)	4	4	4	2
number of antenna at each MS (N_k)	2	2	2	4

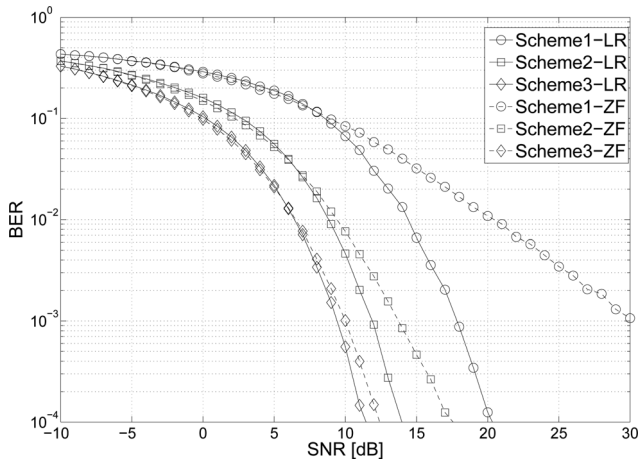


Fig. 4 Average BER against average SNR per symbol for UL transmission when using the LR and ZF detection, respectively

System configuration is shown in Table 1. Furthermore, only a single data stream is transmitted to from each of K MSs to the BS and 16QAM is used

proposed LR scheme over the traditional ZF arrangement is reduced, which is because of the extra receive diversity gleaned.

In Fig. 5, we portray the average BER against average SNR per symbol performance for DL transmissions, when using the VP and ZF precoders. The system configuration is that of Scheme 3 in Table 1. Furthermore, $n_k = 2$ data streams are transmitted to each of the K MSs, where 16QAM is used for the higher eigenvalue, whereas quadrature phase shift keying (QPSK) is used for the lower one. As we can see from Fig. 5, again, the VP-based scheme outperforms the traditional ZF arrangement by about 19 dB at a BER of 10^{-3} .

In Fig. 6, the average UL BER against average SNR per symbol performance is shown for the LR and ZF schemes using Scheme 3 of Table 1. Furthermore, $n_k = 2$ data streams are transmitted from each of the K MSs to the BS, using 16QAM for the higher eigenvalue and QPSK for the lower one. As we can see from Fig. 6, the LR-based scheme outperforms the traditional ZF one by about 15 dB

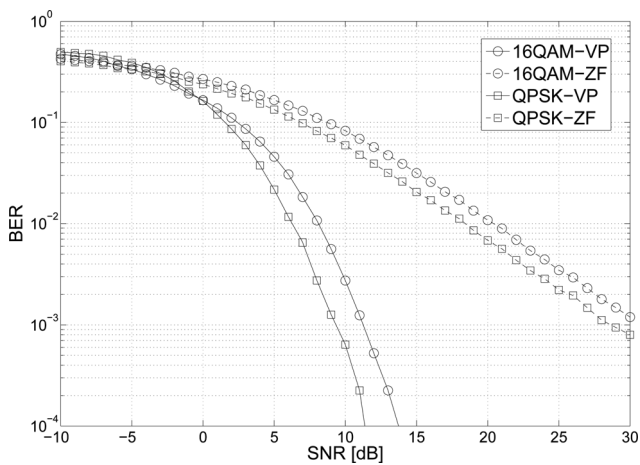


Fig. 5 Average BER against average SNR per symbol for DL transmission when using the VP and ZF precoding, respectively

System configuration is chosen to be Scheme 3 of Table 1. Furthermore, two data streams are transmitted from the BS to each MS, where 16QAM is used for the higher eigenvalue, whereas QPSK for the lower one

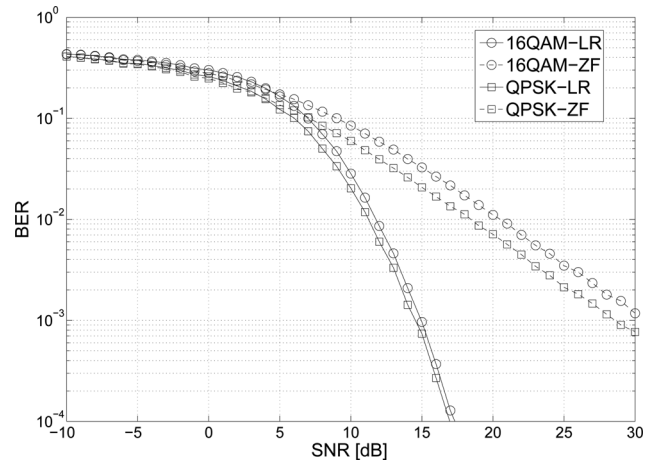


Fig. 6 Average BER against average SNR per symbol for UL transmission when using the LR and ZF detection, respectively

System configuration is chosen to be Scheme 3 of Table 1. Furthermore, two data streams are transmitted from each MS to the BS, where 16QAM is used for the higher eigenvalue, whereas QPSK for the lower one

at a BER of 10^{-3} . Again, this is because the LR-based scheme effectively mitigates the noise enhancement imposed by the traditional ZF receiver.

In Fig. 7, we portray the average BER against average SNR per symbol performance for DL transmissions, when using the VP and ZF precoders. The system configuration is that of Scheme 4 in Table 1. Furthermore, $n_k = 4$ data streams are transmitted to each of the K MSs, where 64QAM is used for the highest eigenvalue, 16QAM is used for the second higher eigenvalue and QPSK is used for the third higher eigenvalue and BSPK for the lowest one. As we can see from Fig. 7, again, the VP-based scheme outperforms the traditional ZF arrangement by about 5 dB at a BER of 10^{-3} for any of the modulation schemes.

In Fig. 8, the average UL BER against average SNR per symbol performance is shown for the LR and ZF schemes using Scheme 4 of Table 1. Furthermore, $n_k = 4$ data streams are transmitted from each of the K MSs to the BS, using 64QAM for the highest eigenvalue, 16QAM for the second higher eigenvalue, QPSK for the third higher eigenvalue and BPSK for the lowest one. As we can see

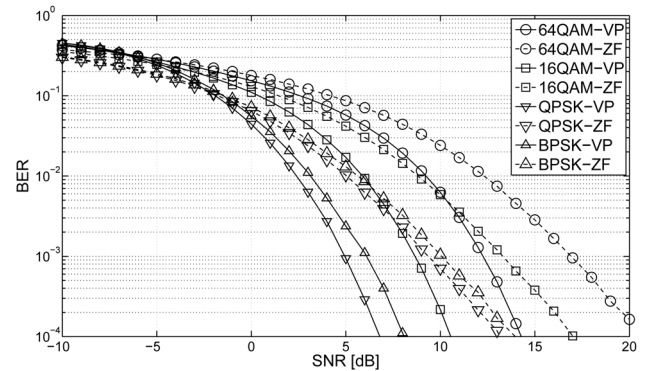


Fig. 7 Average BER against average SNR per symbol for DL transmission when using the VP and ZF precoding, respectively

System configuration is chosen to be Scheme 4 of Table 1. Furthermore, four data streams are transmitted from the BS to each MS, where 64QAM is used for the highest eigenvalue, 16QAM is used for the second higher eigenvalue, QPSK is used for the third higher eigenvalue, whereas BPSK for the lowest one

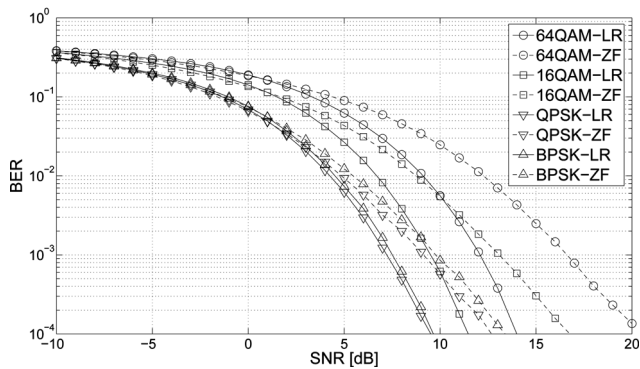


Fig. 8 Average BER against average SNR per symbol for UL transmission when using the LR and ZF detection, respectively

System configuration is chosen to be Scheme 4 of Table 1. Furthermore, four data streams are transmitted from each MS to the BS, where 64QAM is used for the highest eigenvalue, 16QAM is used for the second higher eigenvalue, QPSK is used for the third higher eigenvalue, whereas BPSK for the lowest one

from Fig. 8, the LR-based scheme outperforms the traditional ZF one by about 5 dB at a BER of 10^{-3} .

5 Conclusions

In this treatise, an SVD-based VP-aided DL MUT scheme and an LR-aided UL MUD scheme were proposed. In the proposed DL VP scheme, a perturbation vector was introduced for taking into account the specific modulation schemes assigned to the different-quality eigenbeams of the SVD MUT employed. For the LR-aided UL MUD scheme, our transform is invoked on the composite channel, which can render the symbols distinguishable. In excess of 15 dB SNR gains were attained for both the UL and DL in the investigated scenarios. This is a benefit of mitigating the ZF receiver's noise enhancement in the UL with the aid of LR and that of the DL ZF precoder's limitations with the aid of the VP.

6 Acknowledgments

The financial support of the National Basic Research Program of China (973 Program) (no. 2009CB320404), of the National Natural Science Foundation of China (no. 61072068), of ISN1003002, of the Innovation Fund for returned overseas Scholars of Xidian University (no. 64101879) and of the China 111 Project (no. B08038), of the National Science and Technology Major Project (numbers 2011ZX03005-003-03, 2011ZX03005-004, 2011ZX03004-003), as well as that of the RCUK under the UK-China Science Bridge Initiative in 4G wireless communication is gratefully acknowledged.

7 References

- 1 Telatar, I.E.: 'Capacity of multi-antenna Gaussian channels', *Eur. Trans. Telecommun.*, 1999, **10**, pp. 585–595
- 2 Joham, M., Utschick, W., Nosske, J.A.: 'Linear transmit processing in MIMO communications systems', *IEEE Trans. Signal Process.*, 2005, **53**, pp. 2700–2712
- 3 Spencer, Q.H., Swindlehurst, A.L., Haardt, M.: 'Zero-forcing methods for downlink spatial multiplexing in multiuser MIMO channels', *IEEE Trans. Signal Process.*, 2004, **52**, pp. 461–471
- 4 Liu, W., Yang, L.L., Hanzo, L.: 'SVD-assisted multiuser transmitter and multiuser detector design for MIMO systems', *IEEE Trans. Veh. Technol.*, 2009, **58**, pp. 1016–1021
- 5 Hochwald, B.M., Peel, C.B., Swindlehurst, A.L.: 'A vector-perturbation technique for near-capacity multiantenna multiuser communication-part II: perturbation', *IEEE Trans. Commun.*, 2005, **53**, pp. 537–544
- 6 Shi, S., Schubert, M., Boche, H.: 'Downlink MMSE transceiver optimization for multiuser MIMO systems: MMSE balancing', *IEEE Trans. Signal Process.*, 2008, **56**, pp. 3702–3712
- 7 Wübben, D., Böhnke, R., Kühn, V., Kammeyer, K.D.: 'Near-maximum-likelihood detection of MIMO systems using MMSE-based lattice-reduction'. Proc. IEEE Int. Conf. Communications, Paris, France, June 2004, pp. 798–802
- 8 Yao, W., Chen, S., Hanzo, L.: 'A transceiver design based on uniform channel decomposition and MBER vector perturbation', *IEEE Trans. Veh. Technol.*, 2010, **59**, pp. 3153–3159
- 9 Ma, X., Zhang, W.: 'Performance analysis for MIMO systems with lattice-reduction aided linear equalization', *IEEE Trans. Commun.*, 2008, **56**, pp. 309–318